Spatiotemporal Nonstationary Robust Modeling Between Luojia1-01 Night-Time Light Imagery and Urban Community Average Residence Price

Chang Li, Linqing Zou, Yinfei He, Bo Huang, and Yan Zhao

***Abstract*—This article is the first to propose a novel spatiotemporal nonstationary robust modeling between high spatial resolution Luojia1-01 night-time light intensity (NTLI) and urban community average residence price (UCARP), which encodes the spatiotemporal independent variable NTLI based on a new proposed geographical coding (GeoCode) to enhance the explanatory power of NTLI and leverages geographically and temporally weighted regression (GTWR) based on a new proposed spatiotemporal anomaly detection (STAD) to remove spatiotemporal outliers and then to robustly estimate modeling result. UCARP data and Luojia1-01 NTL imagery obtained from Wuhan, China, in June, September and October 2018 were crawled and downloaded for the experiment, whose results show that GTWR performs better than geographically weighted regression and temporally weighted regression. The comparisons of GTWR with 1) original data; 2) GeoCode (GC); 3) STAD; 4) first STAD last GeoCode (STAD_GC), and 5) first GeoCode last STAD (GC_STAD) show that 1) the q values of geographical detector corresponding to the above methods are 0.055, 0.407, 0.126, 0.666, and 0.671, respectively, during September; 2) the adjusted R^2 values of GTWR are 0.460, 0.488, 0.683, 0.693, and 0.697, respectively; and 3) the proposed spatiotemporal data processing scheme, i.e., GC_STAD, has the most robust and best precision. This article not only proposes a new spatiotemporal nonstationary robust modeling method between small-scale NTL and UCARP but also reveals its underlying mechanism.**

***Index Terms*—Geographical detector (Geodetector), geographical coding (GEOCODE), night-time light intensity (NTLI), spatiotemporal anomaly detection (STAD), spatiotemporal nonstationary robust modeling, urban community average residence price (UCARP).**

I. Introduction

URBAN community average residence price (UCARP) has traditionally played a significant role in the field of urban sociology, regional geography, and social economic investigation [1], [2], [3]. The analysis of the factors influencing urban residence prices has become a research hotspot. Residence prices are a popular metric that scholars pay close attention to, especially in China. The China National Bureau of Statistics' residence price index shows that from 1998 to 2010, residence prices increased by 78%. Residence purchase issues have become the main concern of the public and the government [4]. Numbeo, the world's largest online collaborative database site, ranked "Prices by city of price per square meter to buy residences in city centres," in which residence prices in some Chinese cities were surprisingly higher than those in cosmopolitan metropolises such as New York, Paris, and Tokyo. CBRE's latest Global Living Report: Urban Guidelines in 2019 showed that Hong Kong is still firmly one of the world's most expensive cities, while Shanghai, Shenzhen, and Beijing rank third, fifth, and ninth, respectively. The research on residence prices in China has important practical significance. Among the cities in China, Wuhan, as a typical second-tier city located in central China, is universal and representative in terms of economic development and spatial distribution.

Residence price studies have traditionally been divided into two categories. One category discusses the growth process of urban residence prices over time and estimates residence price changes [5], [6], [7], [8], [9]. The other category analyses the spatial distribution characteristics of residence prices [10], [11], [12], [13]. These models generally discuss the separation of time and space. However, Einstein's theory of relativity suggests that time and space are closely related and inseparable [14]. Temporal data can provide potential information on spatial dynamic processes and be used to predict relevant variables. Considering all of these factors, geographically and temporally weighted regression (GTWR) [15] is creatively proposed, which considers both time and space. Currently, spatiotemporal modeling has been widely studied in the fields of remote sensing (RS) and geographic information science (GIS) [16]. The connection between residence prices and their affecting factors has been studied using GTWR [15], [17], [18], and the best-fitting results were obtained. Literature [19] integrated geographically weighted regression (GWR) and time series to forecast future residence prices. Literature [20] explored a GTWR approach using travel time distance metrics to evaluate residence prices. Literature [21] quantified the impact of built environment on subway rides at spatiotemporal scales using GTWR and found that low

Received 11 June 2024; revised 12 July 2024 and 31 July 2024; accepted 27 August 2024. Date of publication 16 September 2024; date of current version 23 September 2024. This work was supported in part by the National Natural Science Foundation of China under Grant 41771493 and Grant 41101407 and in part by the Fundamental Research Funds for the Central Universities under Grant CCNU22QN019. *(Corresponding author: Chang Li.)*

Chang Li is with the Key Laboratory for Geographical Process Analysis & Simulation of Hubei Province, Wuhan 430079, China, and also with the College of Urban and Environmental Science, Central China Normal University, Wuhan 430079, China (e-mail: lcshaka@126.com).

Linqing Zou is with the School of Remote Sensing and Information Engineering, Wuhan University, Wuhan 430079, China (e-mail: zoulinqing@whu.edu.cn).

Yinfei He and Yan Zhao are with the College of Urban and Environmental Science, Central China Normal University, Wuhan 430079, China.

Bo Huang is with the Department of Geography, The University of Hong Kong, Hong Kong (e-mail: bohuang@hku.hk).

Digital Object Identifier 10.1109/JSTARS.2024.3456376

residence prices in the suburbs increased resident subway travel needs in the area. How factors influencing residence are associated with residence prices in Shenzhen is studied in [22]; Wu et al. further analyzed their temporal and spatial variation using multiscale GTWR. Zhou et al. [23] researched the influential factors of residence prices and rental prices from supply and demand and explored spatial-temporal heterogeneity based on the GTWR model. The spatial and temporal differentiation of residence prices in city infrastructure is explored [24]. However, all of these published articles estimated residence prices using multiple variables, in that many factors that affect residence prices exist. Actually, multiple variables can lead to inconsistent standards (e.g., different factors) of modeling residence prices. Whether we can find a comprehensive index and a unified standard to estimate residence prices is worth studying. Hence, we review factors affecting residence prices below.

Currently, related studies show that urban residence prices correlate with the following:

1) GDP-led economic factors [25], [26], [27], [28], such as household income [29], [30], [31], taxes [32], [33], rent [34], [35], and the employment rate;
2) population (POP) factors, such as POP density and total POP [36], [37], [38];
3) spatial distribution factors, such as land value [39], [40], [41], accessibility to green space [13], [42], public transit [43], [44] and central business district [45], [46];
4) urbanization (URB) [47], [48], [49].

However, many explanatory variables are used to determine residence prices in current studies, which may lead to 1) over-parameterization and 2) correlation between independent variables (i.e., multicollinearity). Literature [50] solved these two problems and studied the factors influencing residence prices on a spatial scale but did not consider the time-series influence. Whether it is possible to explore a comprehensive indicator and a unitary standard that can represent all factors influencing residence prices in both time and space (i.e., spatiotemporal) scales has important theoretical research value and practical application significance.

Recently, night-time light RS technology has given researchers a new approach for analyzing URB and urban problems. Research [51], [52], [53], [54], [55] shows that NTLI is positively related to human activity, and high correlations between night-time light data and GDP [56], [57], [58], [59], POP density [60], [61], and power consumption [62], [63] exist. Night-time light data can be used as a comprehensive indicator of regional socio-economic activities [64], [65], [66], [67], [68], [69], [70]. These data have been widely used in URB [71], [72], [73], urban-rural differentiation [74], socio-economic parameter estimation [75], [76], and light pollution detection [77], [78] studies. The Traditional Defense Meteorological Satellite Program—Operational Linescan System and the Suomi National Polar-orbiting Partnership—Visible Infrared Imaging Radiometer images have resolutions of 1000 and 500 m, respectively [79]. The image resolution limitation requires research on residence prices based on night-time light data and must primarily comprise cities or provinces as the research units. However, small-scale aspects, such as loops, administrative divisions, and transportation, all of which have high spatial heterogeneity, influence urban residence prices. Image resolution restricts existing research since it often ignores spatial information. The Luojia1-01 satellite—the first night-time light RS satellite in the world with a spatial resolution of 130 m—has a higher resolution than other night-time light satellites. Therefore, the high spatial resolution of Luojia1-01 data can provide more accurate night-time light sources and rich spatial information [76], [80], making it possible to study urban interior residence prices on a microscopic scale. Li et al. [50] researched the potential for using high spatial resolution Luojia1-01 images as a comprehensive variable for estimating residence prices using the spatial dimension. However, the variation in community average residence prices compared with night-time light usage over time was neglected.

In general, no reported literature has used a comprehensive single variable to estimate residence prices from a spatiotemporal perspective at a small scale. Additionally, no reported literature has used geographical coding (GeoCode)-based night-time light intensity (NTLI) to estimate and model residence prices. More specifically, central urban areas and suburbs may have the same NTLI, but in fact, the economic levels of the two differ so greatly that their residence prices may widely vary. Hence, if NTLI is used to model residence prices directly, the explanatory power of independent variables on NTLI is not very strong. Moreover, the issue of detecting spatiotemporal anomalies should be taken into account when modeling residence price. To solve the aforementioned issues and take advantage of the high spatial resolution Luojia1-01 satellite, we originally propose a novel spatiotemporal nonstationary robust modeling method that leverages the GeoCode detector and spatiotemporal anomaly detection (STAD) for robustly modeling UCARP using Luojia1-01 imagery and quantitatively explore the impact of different execution sequences of GeoCode and STAD on the results. The innovations and contributions of this article are as follows.

1) Luojia1-01 NTLI is introduced to the spatiotemporally model and analyze UCARP as a single variable, namely, a comprehensive indicator and a unitary standard, at small scales for the first time. Currently, no relevant literature on spatiotemporal modeling and analyzing UCARP using Luojia1-01 imagery exists.
2) A GeoCode method, which is different from geocoding in the GIS, is uniquely proposed to improve the explanatory power of NTLI and the precision of spatiotemporal modeling for UCARP. Through GeoCode that is similar to the encoder processing in the autoencoder (AE), additional spatial details (i.e., spatial economic differences) of NTLI, related to price-related elements, are enhanced to improve modeling precision.
3) An STAD method is proposed to remove spatiotemporal anomaly data (i.e., outliers). Through hotspot and overlay analyses of the spatiotemporal NTLI and UCARP data, anomaly data (gross errors) are eliminated to provide a high-quality data source for robust modeling;
4) The geographical detector (Geodetector) is proposed to detect the explanatory power of different spatial

independent variables, which helps select the best spatial independent variable.

5) An NTL data processing flow for GTWR is proposed for the first time and offers a quantitative comparison of the impact of different execution sequences of GeoCode and STAD on the results. The spatiotemporal data processing scheme of the first GeoCode last STAD data (GC_STADD) ultimately provides the best regression results by comparing data with and verifying results against the original data, GeoCode data (GCD), STADD, and first STAD last GCD (STAD_GCD);
6) The spatial-temporal nonstationary coupling mechanism between small-scale NTLI and UCARP is shown from the perspectives of the urban loop line, infrastructure development, POP density, etc., for the first time.

II. Theory and Methodology

In this article, the community NTLI from Luojia1-01 is used as a single explanatory variable and a unified standard to estimate the dependent variable UCARP. The reasons for using this method are as follows.

1) Night-time light data has comprehensive characteristics. According to the literature review in the introduction, functional relationships between UCARP and GDP, POP, spatial distribution, and URB exist; thus, formula (1) is obtained. Moreover, functional relationships between NTLI and GDP, POP, spatial distribution, and URB exist; thus, formula (2) is obtained. Formula (3) is derived from combining the two formulas. A compound functional relationship F conclusively exists between UCARP and NTLI. Therefore, night-time light data can be used as a comprehensive indicator to evaluate factors related to residence prices

$$\mathrm{UCARP} = f\left(\mathrm{GDP}, \mathrm{POP}, \mathrm{SD}, \mathrm{URB}\right) \tag{1}$$

$$\begin{cases} \mathrm{GDP} = g_1(\mathrm{NTLI}) \\ \mathrm{POP} = g_2(\mathrm{NTLI}) \\ \mathrm{SD} = g_3(\mathrm{NTLI}) \\ \mathrm{URB} = g_4(\mathrm{NTLI}) \end{cases} \tag{2}$$

$$\begin{aligned} &\mathrm{UCARP} \\ &\quad = f\left(g_1\left(\mathrm{NTLI}\right), g_2\left(\mathrm{NTLI}\right), g_3\left(\mathrm{NTLI}\right), g_4\left(\mathrm{NTLI}\right)\right) \\ &\quad = F\left(\mathrm{NTLI}\right). \end{aligned} \tag{3}$$

2) Luojia1-01 data have a microscale representation. While the data have a higher resolution than traditional night-time light data, these microscopic night-time light characteristics can provide more spatial details related to residence price-related elements. GeoCode is proposed to enhance these detailed spatial attributes in NTLI. Through GeoCode, spatial economic differences of NTLI, which reflect UCARP, are adjusted by coding NTLI to improve the explanatory power of the independent variable.

In the experimental section, we compare many methods to verify the best results. The smoothest technical flow of the proposed spatiotemporal processing for GTWR is shown in Fig. 1 and is further elaborated as follows.

1) Luojia1-01 data preprocessing. The radiometric values of the data are converted to NTLI data. The formula for converting the radiometric brightness from Luojia1-01 data is as follows:

$$\mathrm{NTLI} = \mathrm{DN}^{3/2} \times 10^{-10} \tag{4}$$

where NTLI is the radiometric value after absolute radiometric correction, the unit is $\mathrm{W}/(\mathrm{m}^2 \cdot \mathrm{sr} \cdot \mu\mathrm{m})$, and DN is the gray value of the image.

2) UCARP data obtaining and processing. Crawler technology is used to obtain residence data from Wuhan communities using real estate networks, such as "Lianjia" and "Anjuke." The crawled data are cleaned, and anomaly and invalid data are eliminated. UCARP vector data are obtained by combining the crawled community attribute data and the corresponding vector data through their collective attributes, i.e., community name, and location.
3) UCARP and NTLI overlaid with vector data. UCARP data are overlaid with multitemporal Luojia1-01 images. Then, the community vector dataset with both NTLI and UCARP attributes is obtained.
4) GeoCode. The average NTLI (ANTLI) is calculated for each municipal district of the city, and the district GeoCode factor M_j is obtained by sorting the ANTLI values of municipal districts in ascending order. We consider spatial differences in UCARP between different districts within a city by geographically coding NTLI.
5) GeoCode-based NTLI (GeoNTLI). The hierarchical method is used to discretize the NTLI of all communities, and then the discretized NTLI values (i.e., D_NTLI) are obtained. Combined with the regional coding factor M_j, the night light discretization value combined with geographical information, GeoNTLI, is obtained based on district geocoding. It is worth noting that $(\mathrm{NTLI})_i$ is assumed not to be equal to 0 due to community residence.
6) STAD. First, hotspot analysis is performed on the spatiotemporal UCARP and GeoNTLI data. Then, clustering and outlier analysis is used to identify the high–high and low–low clusters of UCARP. Overlay analysis is used to identify the common clustering locations of GeoNTLI and UCARP. Communities where UCARP and GeoNTLI have no similar clustering (such as communities with high UCARP and low NTLI, or the opposite) are considered anomaly data and are eliminated. Finally, the reliable or robust GeoSTAD_NTLI data are obtained by the aforementioned GC_STADD processing.
7) Geodetection of explanatory power. The explanatory power of different independent variables (e.g., NTLI, GeoNTLI, GeoSTAD_NTLI, and data obtained with other methods) on the dependent variable UCARP is explored by Geodetector.
8) GTWR modeling. The model is established using GeoSTAD_NTLI as the independent variable. Considering spatiotemporal heterogeneity (i.e., nonstationarity), the spatiotemporal information is integrated into the

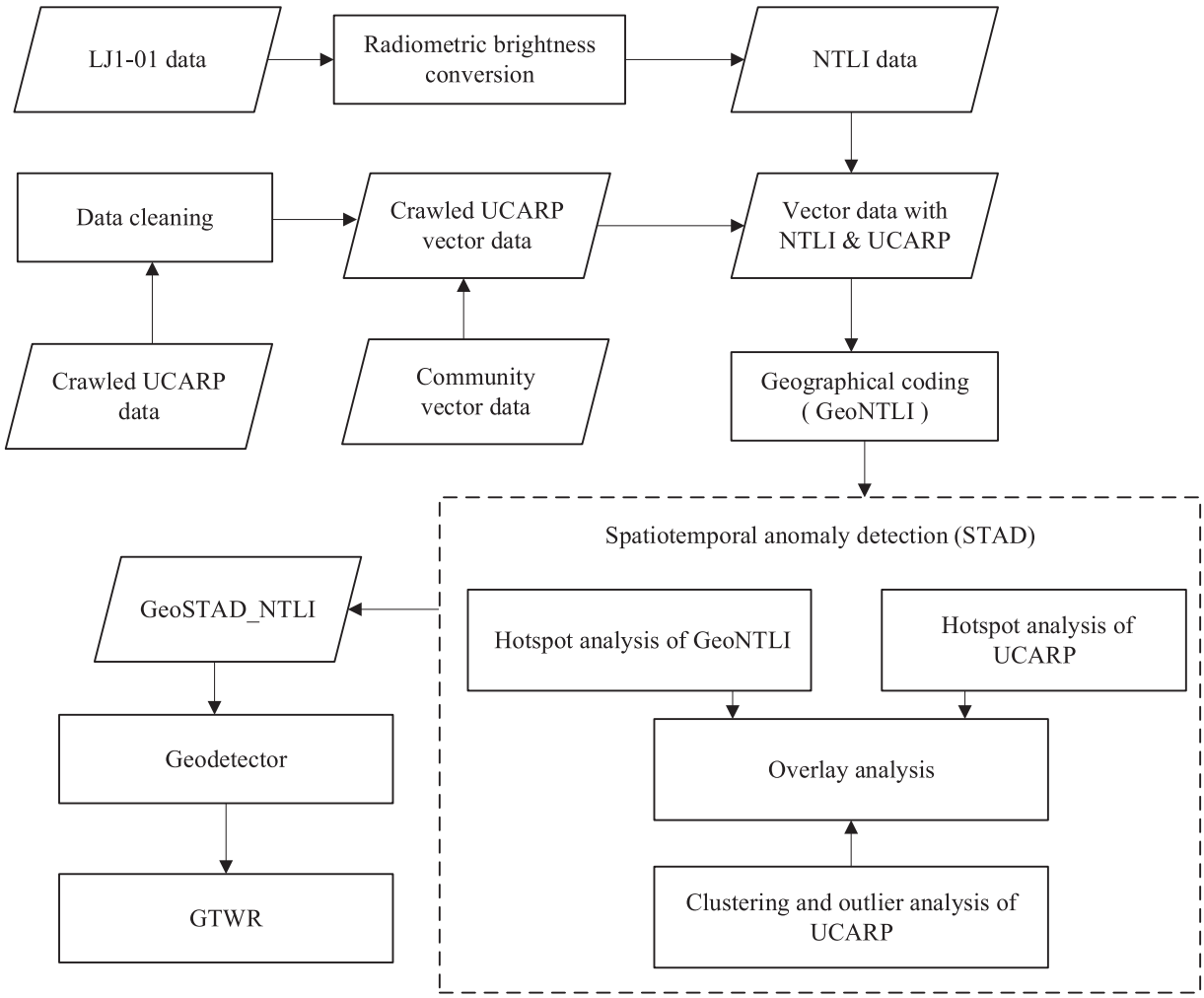

Fig. 1. Technology roadmap of the proposed spatiotemporal processing method for GTWR.

weighted matrix to control the spatiotemporal nonstationarity between UCARP and GeoSTAD_NTLI.

It should be noted that different execution orders (i.e., STAD_GCD and GC_STADD) can lead to changes in spatiotemporal modeling accuracy. Therefore, it is particularly important to compare the accuracy of the two and analyze the reasons behind it. The following sections explain and introduce some key technologies.

A. Geographical Coding

Unlike geocoding which is the process of transforming a description of a location to a location on the earth's surface, GeoCode proposed in this article means to encode and adjust NTLI to reflect UCARP differences between the districts of a city and improve the explanatory power of NTLI. First, the ANTLI of each district is calculated using formula (5), and then the district GeoCode factor M_j is obtained by sorting the values of ANTLI in ascending order

$$(\mathrm{ANTLI})_j = \left(\sum_{i=0}^{k} (\mathrm{NTLI})_i \times n_i\right) \Big/ S_j \quad (i = 0, 1, \ldots, k, j = 1, 2, \ldots m) \tag{5}$$

where *j* represents the coding number of each municipal district in a city; *m* represents the number of districts in a city; *k* represents the number of pixels in the *j*th district; $(\mathrm{ANTLI})_j$ represents the ANTLI of the *j*th district; $(\mathrm{NTLI})_i$ represents the NTLI of the *i*th pixel in the district; n_i represents the area of the *i*th pixel; and S_j represents the area of the *j*th municipal district.

Using the above formula, the ANTLI of each district can be obtained, and the ANTLI of each district can be sorted from low to high (representing the economic level from low to high). The sequence number of each district is the coding factor M_j of each district.

The geographic detector requires categorical explanatory variables, so it is necessary to use classification methods to discretize explanatory variables. Commonly used data discretization methods include cluster analysis (such as *K*-Means), classification analysis, equal interval grading, and equal percentage grading. Because NTLI is floating-point data after absolute radiometric correction, the equal percentage classification method is used to discretize the floating-point NTLI to 10 levels from

0 to 9 to acquire the discretized NTLI value D_NTLI with unit $\mathrm{W}/(\mathrm{m}^2 \cdot \mathrm{sr} \cdot \mu\mathrm{m})$.

With different spatial distributions of each district existing in a large city, certain differences in the level of economic development also exist, and overall differences between UCARP occur in each district. In addition, some districts belong to the central part of the city, while others are located on the outskirts of the city. The loop line information (the second ring and the third ring) is buried between the central part of the city and the outskirts of the city. Therefore, the district GeoCode factor of the independent variable (i.e., NTLI), which is similar to the encoder processing in the AE, can effectively divide the space to improve the explanatory power of the independent variable.

To increase the explanatory power of independent variables, the GeoCode detector is proposed. It adds the geocoding factor M_j to the D_NTLI of different districts after discretizing the explanatory variables. The interpretation variables based on GeoCode are calculated as follows:

$$(\mathrm{GeoNTLI})_i = M_j \times 10^{\lceil |\lg((\mathrm{D\_NTLI})_i + 0.1)| \rceil} + (\mathrm{D\_NTLI})_i \quad i = 1, 2, \ldots, n \quad j = 1, 2, \ldots, m \tag{6}$$

where the *i*th located community belongs to the *j*th district; $(\mathrm{GeoNTLI})_i$ is the discretized NTLI based on GeoCode; M_j is the GeoCode factor of the *j*th district, that is, the ascending sorted number (which can reflect the economic level) of each district; and $(\mathrm{D\_NTLI})_i$ is the discretized NTLI obtained by using the hierarchical method for NTLI. It is worth noting that $(\mathrm{NTLI})_i \neq 0$ in this article; $\lceil\ \rceil$ is a rounding-up function that adds 1 to the integer as long as a decimal is present; $||$ represents the absolute value; and lg represents the base-10 logarithm.

B. Spatiotemporal Anomaly Detection

1) STAD is proposed to eliminate anomaly data by first using hotspot analysis and then overlay analysis of spatiotemporal data.
2) Time-series-based hotspot analysis uses Getis-Ord G_i^* statistics to identify hotspots and cold spots with statistical significance; these are performed for both UCARP and GeoNTLI.
3) Time-series-based clustering and outlier analysis identify different UCARP and GeoNTLI clustering types.
4) Spatiotemporal overlay analysis identifies the common clustering space of UCARP and GeoNTLI and the high-high and low-low clusters of UCARP by intersection processing for the above time-series results. Spatiotemporal anomaly data with different clustering spaces and other types of clustering are detected and eliminated at different timepoints, so that robust GeoSTAD_NTLI is obtained.

Generally, the higher the NTLI value is, the more concentrated the POP; the higher the POP density is, the higher the level of economic development; the better the infrastructure development is, the higher the residence price. However, in reality, areas may exist where NTLI is high but the residence price is low, or NTLI is low and the residence price is high. For example, some suburbs have villas that have low building density and small quantity. Their lights are darker than those in the main urban area, but their residence prices (e.g., a luxury villa) may be significantly higher than those of other suburban buildings. The main urban areas may also have some older communities that have lower residence prices than those in surrounding communities. Because the main urban area is densely populated, and the infrastructure is evenly distributed, these low-price communities have NTLI values similar to those of other communities. Such anomalous data seriously affect modeling precision, so data cleaning (i.e., gross error detection) is needed. Therefore, by overlaying spatial hot and cold areas of different time phases, these anomalous (contradictory) data can be removed using overlay analysis with intersection and provide high-quality data sources for robust UCARP modeling and thus improve modeling precision.

C. Geographical Detector for GeoCode

Geodetector is a statistical method proposed by [81] to measure the spatial differentiation of geographic objects and reveal the driving forces behind them.

Geodetector includes a risk detector, factor detector, ecological detector, and interaction detector, which quantitatively express the spatial heterogeneity of residence prices from four different perspectives as well as the ability of night-time light to influence the spatial differentiation of UCARP. Among them, the factor detector can detect the explanation degree of night-time lights on the spatial differentiation of UCARP, which is expressed by the q value

$$q = 1 - \left(\sum_{h=1}^{L} N_h \sigma_h^2\right) \Big/ \left(N\sigma^2\right). \tag{7}$$

The q value satisfies the noncentral F distribution

$$F = \frac{N-L}{L-1}\frac{q}{1-q} \sim F\left(L-1, N-L; \lambda\right) \tag{8}$$

$$\lambda = \frac{1}{\sigma^2}\left[\sum_{h=1}^{L} \bar{Y}_h^2 - \frac{1}{N}\left(\sum_{h=1}^{L} \sqrt{N_h}\bar{Y}_h\right)^2\right] \tag{9}$$

where λ is a noncentral parameter and $\bar{Y}_h$ is the mean of the *h*th stratification. In formula (8), the significance of the q value can be found by looking up the table.

D. Spatiotemporal Modeling

The GTWR model provides a specific calculation method for the spatiotemporal weighted matrix to solve the problem of spatiotemporal nonstationarity. The mathematical expression of the state-of-the-art GTWR model based on spatiotemporal processing is as follows:

$$(\mathrm{UCARP})_i = \beta_0\left(u_i, v_i, t_i\right) + \beta_1\left(u_i, v_i, t_i\right)(\mathrm{GeoSTAD\_NTLI})_i + \varepsilon_i, i = 1, 2, \ldots, n \tag{10}$$

where $(\mathrm{UCARP})_i$ is the residence price of community *i*; *n* is the number of communities; (u_i, v_i, t_i) represents the coordinates of community *i*; t_i indicates the time coordinate of community

i; $\beta_0(u_i, v_i, t_i)$ is the spatiotemporal intercept term of community i; $\beta_1(u_i, v_i, t_i)$ is the regression coefficient of community i, which varies with space and time; $(\text{GeoSTAD\_NTLI})_i$ is processed by GC_STADD; and $\varepsilon_i \sim N(0, \sigma^2)$ is the random error of community i, which satisfies normal distribution. The mathematical expectation is 0, and the variance is σ^2.

The coefficient vector $\hat{\boldsymbol{\beta}} = [\beta_0(u_i, v_i, t_i),\ \beta_1(u_i, v_i, t_i)]^{\mathrm{T}}$ can be expressed as

$$\hat{\boldsymbol{\beta}} = \left(\mathbf{X}^{\mathrm{T}}\mathbf{W}\left(u_i, v_i, t_i\right)\mathbf{X}\right)^{-1}\mathbf{X}^{\mathrm{T}}\mathbf{W}\left(u_i, v_i, t_i\right)\mathbf{P} \tag{11}$$

where the coefficient matrix $\mathbf{X}$ and the dependent variable vector $\boldsymbol{P}$ are

$$\mathbf{X} = \begin{bmatrix} 1 & (\text{GeoSTAD\_NTLI})_1 \\ \vdots & \vdots \\ 1 & (\text{GeoSTAD\_NTLI})_n \end{bmatrix}, \mathbf{P} = \begin{bmatrix} (\text{UCARP})_1 \\ \vdots \\ (\text{UCARP})_n \end{bmatrix} \tag{12}$$

and $\mathbf{W}$ is a spatiotemporal weighted matrix and is explained as follows: measuring spatiotemporal proximity assumes that a point close to the community i in the spatiotemporal coordinate system has a greater influence on the estimation of the coefficient $\beta_1(u_i, v_i, t_i)$ than a point that is distant from the community i. In the spatiotemporal coordinate system, it is assumed that the neighboring community $i(u_i, v_i, t_i)$ is community $j(u_j, v_j, t_j)$, $j = \{1, 2, \ldots, n\}\,(j \neq i)$. According to the GTWR formula, the spatiotemporal distance D_{ij}^{ST} from community i to community j can be calculated as

$$\left(D_{ij}^{ST}\right)^2 = \left[(u_i - u_j)^2 + (v_i - v_j)^2\right] + \tau(t_i - t_j)^2 \tag{13}$$

where τ is a spatiotemporal parameter used to enhance or reduce the effect of the time dimension on the spatial dimension. Then, the kernel function of GTWR can be written as

$$W_{ij} = \exp\left[-D_{ij}^2 \Big/ \left(h^{ST}\right)^2\right]. \tag{14}$$

The mathematical expression AICc for the optimal time and space factor selection of the spatiotemporal weighted regression model is

$$\text{AICc} = 2n\ln(\hat{\sigma}) + n\ln(2\pi) + n\left[(n + \text{tr}(\mathbf{S}))/(n - 2 - \text{tr}(\mathbf{S}))\right] \tag{15}$$

where $\mathbf{S}$ is the hat matrix, subscript c is the estimated value of the modified AIC, $\hat{\sigma}$ is the standard deviation of the error estimate, and $\text{tr}(\mathbf{S})$ is the trace of matrix $\mathbf{S}$.

Furthermore, GWR and temporally weighted regression (TWR) become special cases of GTWR, corresponding to only the spatial weight and temporal weight, respectively.

III. Experimental Results and Analysis

A. Study Area

Wuhan city—the centermost city in central China—is the capital of Hubei Province. Wuhan is located at 113° 41′ E∼115° 05′ E, 29° 58′ N∼31° 22′ N and has a land area of 8569.15 km^2. It covers 15 municipal districts, which are shown in Fig. 2. Wuhan has a radius of 1000 km from its center, covers 1 billion people, and produces 90% of the country's economic output.

We selected Wuhan as our study area for following reasons.

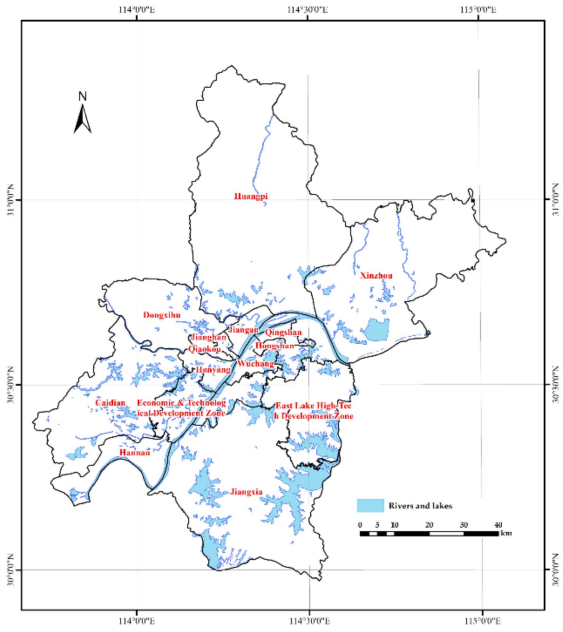

Fig. 2. Wuhan administrative divisions.

1) Wuhan is a modern metropolis and is a representative second-tier city in urban size, economic level, development model, and residence price growth.
2) Its development is mainly internally driven and differs from first-tier cities, such as Beijing, Shanghai, Guangzhou, and Shenzhen, which are driven by powerful national policies and foreign capital.
3) Wuhan has a unique geographical distribution (compared to a typical multicenter city). The Yangtze River and its largest tributary, Hanshui, meet in Wuhan's urban area, forming a unique pattern out of the three towns of Hankou, Wuchang, and Hanyang. This pattern accurately shows how spatial factors impact residence prices.

B. Data

1) Luojia1-01 Data: Luojia1-01, which has a spatial resolution of 130 m, is a new night-time light RS satellite. Fig. 3 shows 12 Luojia1-01 night-time light images covering Wuhan that were obtained in June, September, and October 2018. NTLI value, which is between 0 and 0.1254, is calculated by formula (4).

2) UCARP Data: UCARP data, which cover a wide range of areas and have high timeliness, were acquired from real estate information networks using the "Lianjia" and "Anjuke" web browsers.

The information, including name, unit price, latitude, and longitude of the community, was obtained using Lianjia and Anjuke. We averaged monthly average residence prices in the community by combining the Lianjia and Anjuke data; the resulting data were used as the dependent variable.

As seen in Fig. 4, the obtained 2349 community vector data of 15 districts in Wuhan contains community names, location information, boundaries, etc. Hence, we can link two types of

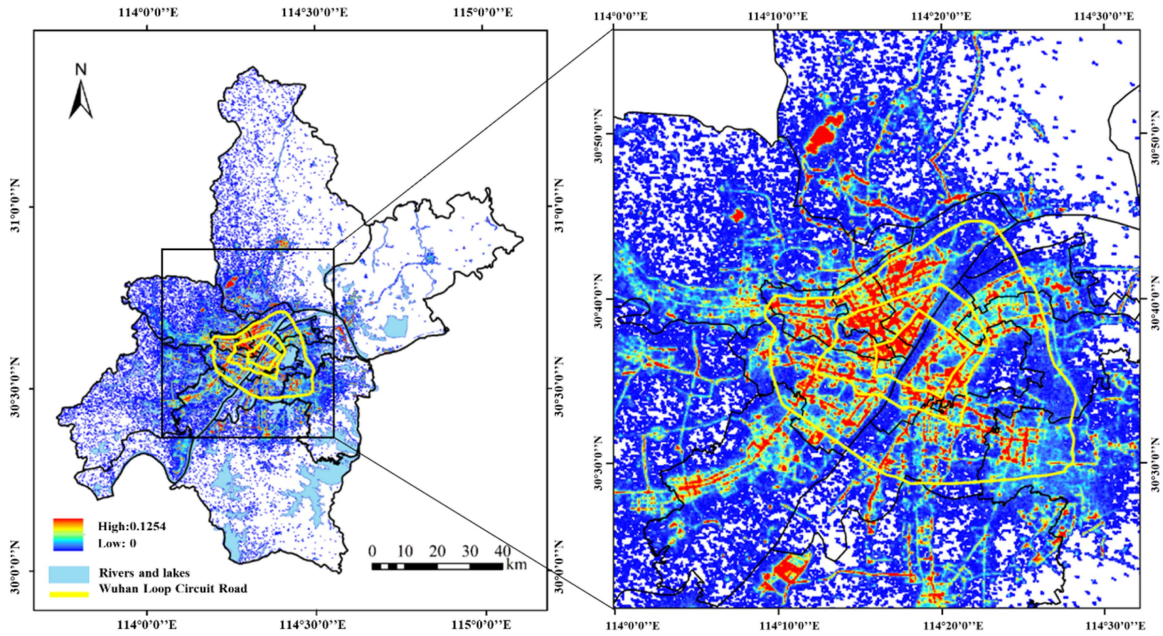

Fig. 3. Luojia1-01 night-time light imagery (NTLI) from Wuhan obtained in June 2018 and calculated by formula (4).

data (i.e., the crawled UCARP data and community vector data) by their common attributes (i.e., community name and location).

C. Experimental Design

Based on the data obtained in varying steps and sequences, some comparative experiments are designed to test which experimental processing yields the best results. Five kinds of data are processed: OD, GCD, STADD, STAD_GCD, and GC_STADD. A comparison of these five data types with Geodetector and three regressions (i.e., GWR, TWR, and GTWR) is conducted to find the best experimental processing.

D. Results

1) GeoCode: The codes M_j representing each district in Wuhan are sorted by the ANTLI of each district from June to October calculated by formula (5) and are shown in Fig. 5 and Table I.

2) Spatiotemporal Anomaly Detection: Spatiotemporal hotspot analysis, clustering and outlier analysis, and overlay analysis of UCARP and GeoNTLI in Wuhan are carried out, and the results are shown in Figs. 6–8. The time-series-based results from June, September, and October show that

1) the hotspots (with variable confidence greater than 90%) of UCARP and GeoNTLI and the high-high clusters of UCARP are concentrated in the city center;
2) the cold spots (with variable confidence greater than 90%) of UCARP and GeoNTLI and the low-low clusters of UCARP are distributed in the periphery, forming a circular structure;
3) the transition zone between the urban center and the outskirts is not significant (i.e., with confidence is less than 90%);
4) overlay analysis of the above time-series-based results can remove the spatiotemporal anomaly effectively using intersection processing.

TABLE I
DISTRICT GEOCODE RESULTS

District name	M_j	District name	M_j
Xinzhou	1	Hongshan	9
Caidian	2	Qingshan	10
Jiangxia	3	Hanyang	11
Huangpi	4	Jiangan	12
Hannan	5	Qiaokou	13
Dongxihu	6	Wuchang	14
East Lake High-Tech Development Zone	7	Jianghan	15
Economic and Technological Development Zone	8		

3) Geodetector Test Results: Table II shows the q value obtained by the factor detector, and Fig. 9 shows the explanatory power for the different processing methods used. According to the test results

1) September's q values for STAD_GCD and GC_STADD are 0.666 and 0.671, respectively;
2) the q values for GCD and STADD increase by 0.352 and 0.071, respectively, compared to OD;
3) the two GeoCode results increase the NTLI explanation for UCARP by 0.352 and 0.540, respectively;
4) the two STAD results increase the NTLI explanation for UCARP by 0.071 and 0.264, respectively.

The results show that

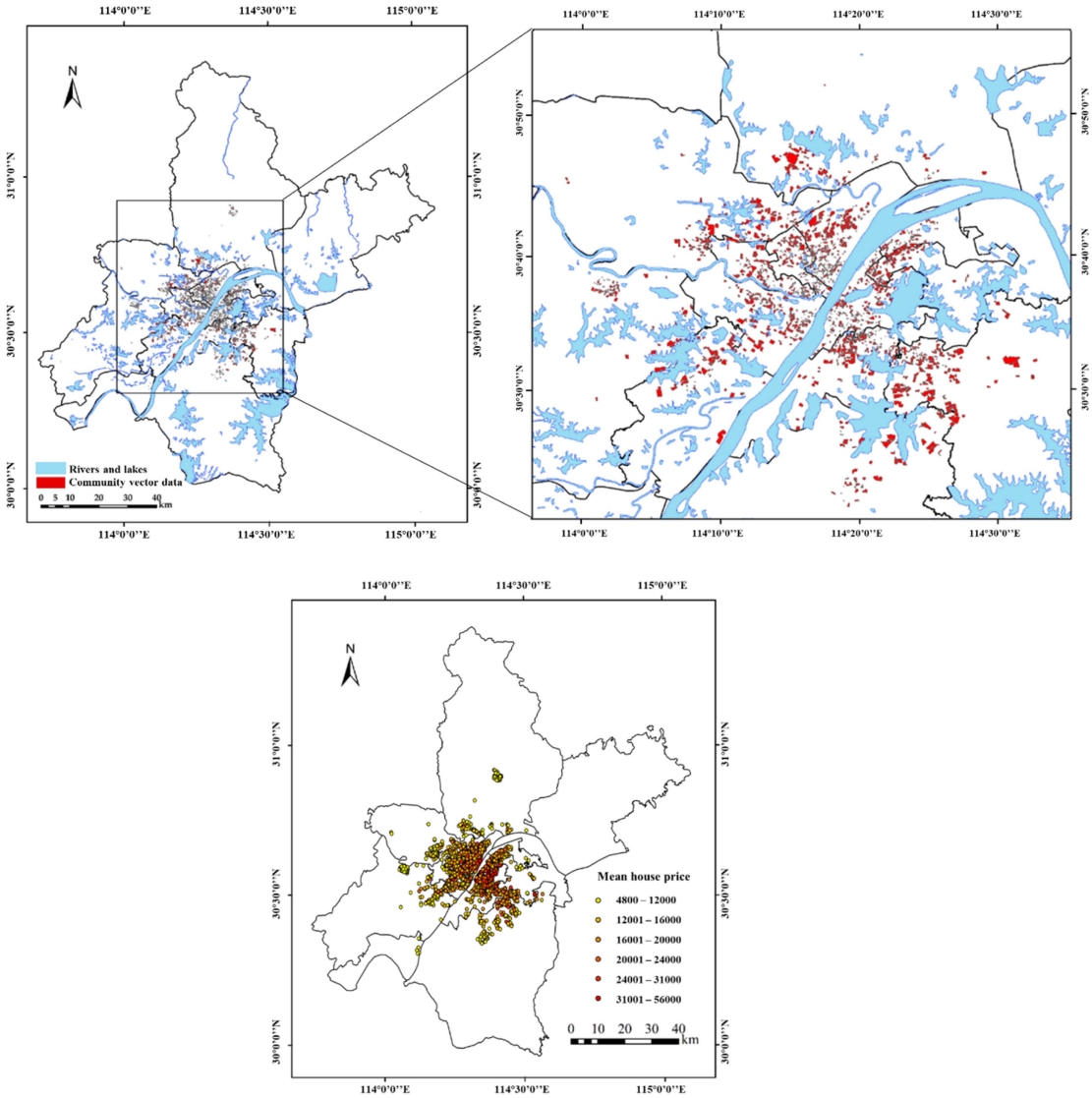

Fig. 4. Community vector and UCARP dataset.

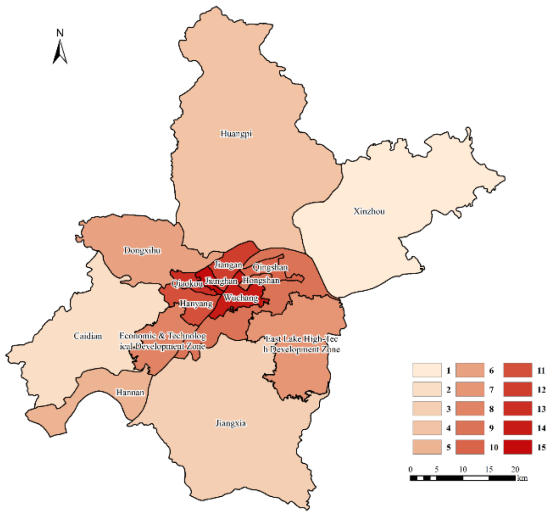

Fig. 5. The GeoCode M_j derived from district geocoding in Wuhan city.

1) NTLI can explain up to 67.069% of UCARP spatial differentiation;
2) both GeoCode and STAD more accurately explain NTLI related to UCARP;
3) GeoCode explains the correlation more accurately than STAD;
4) ultimately, that a statistically significant correlation between NTLI and UCARP exists.

The research method used to detect the relationship between night-time light and residence prices from the perspective of geospatial differentiation has practical reference value and can be applied to the analysis of other residence price-related factors.

4) Geodetector Test Results: Table II shows the q value obtained by the factor detector, and Fig. 9 shows the explanatory power for the different processing methods used. According to the test results

1) September's q values for STAD_GCD and GC_STADD are 0.666 and 0.671, respectively;

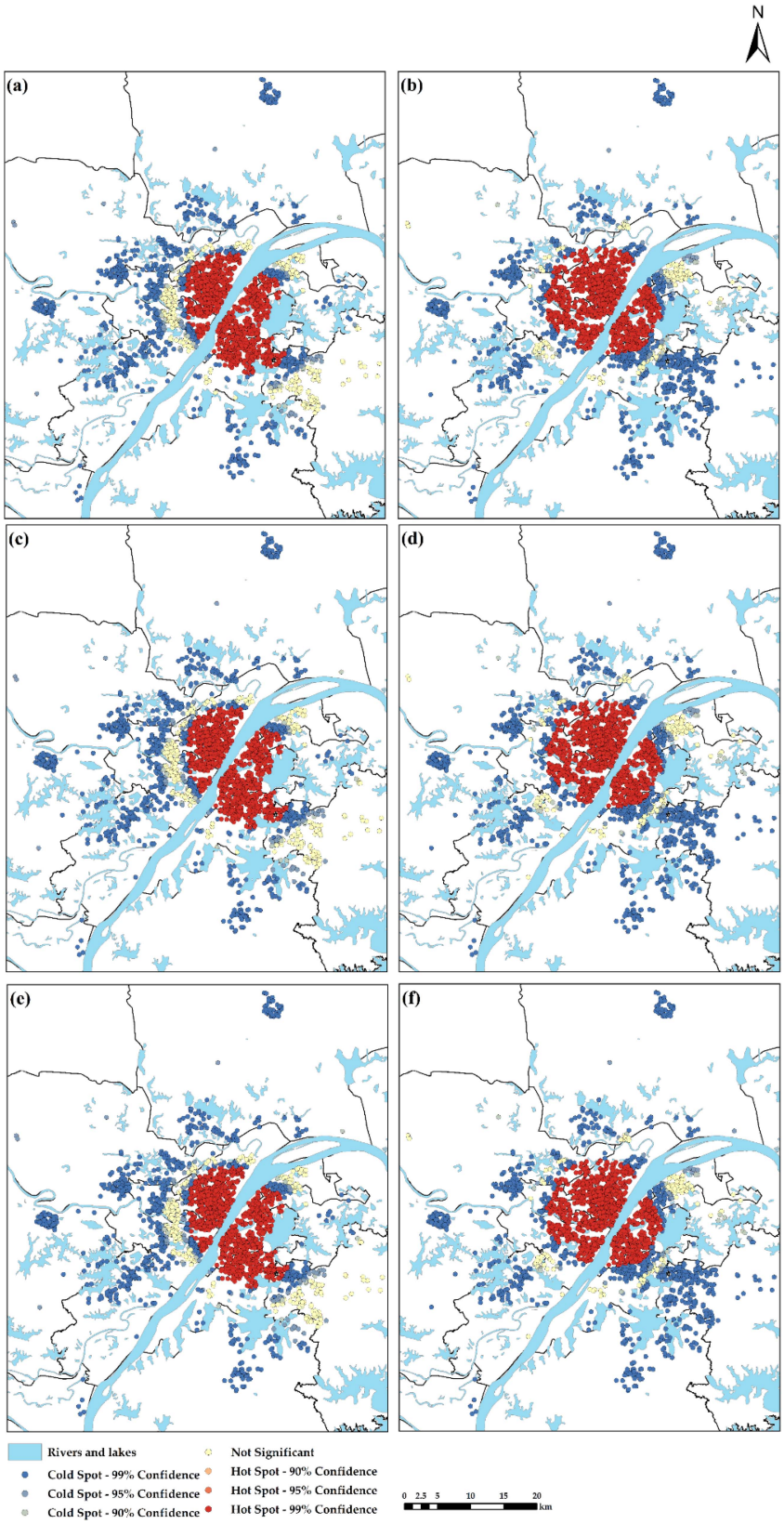

Fig. 6. Time-series-based hotspot analysis of the (a) UCARP in June, (b) GeoNTLI in June, (c) UCARP in September, (d) GeoNTLI in September, (e) UCARP in October, and (f) GeoNTLI in October.

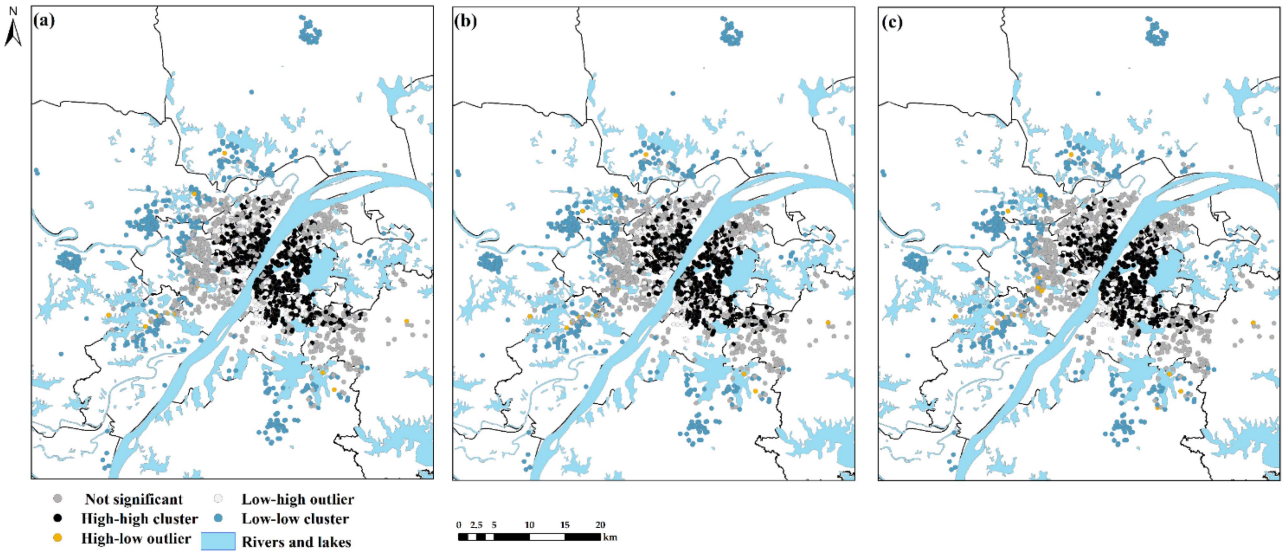

Fig. 7. Time-series-based clustering and outlier analyses of UCARP (a) in June, (b) in September, and (c) in October.

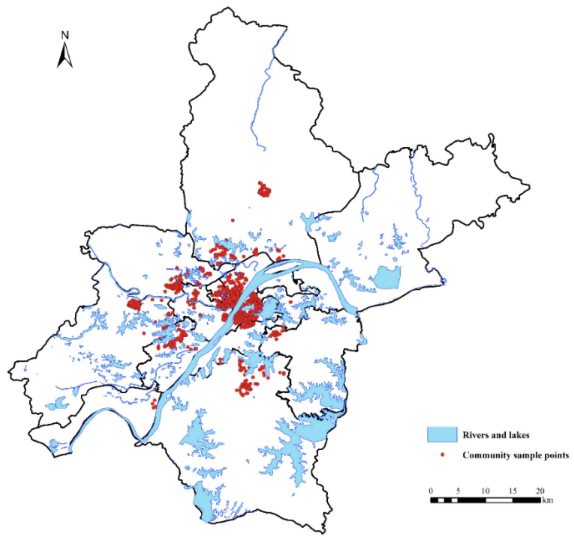

Fig. 8. Results from the spatiotemporal overlay analysis of the above time-series-based results.

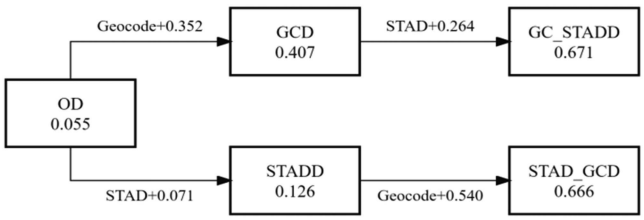

Fig. 9. The explanatory power of varying data processing methods (using the spatial data from September as an example).

2) the q values for GCD and STADD increase by 0.352 and 0.071, respectively, compared to OD;
3) the two GeoCode results increase the NTLI explanation for UCARP by 0.352 and 0.540, respectively;
4) the two STAD results increase the NTLI explanation for UCARP by 0.071 and 0.264, respectively.

The results show that

1) NTLI can explain up to 67.069% of UCARP spatial differentiation;
2) both GeoCode and STAD more accurately explain NTLI related to UCARP;
3) GeoCode explains the correlation more accurately than STAD;

TABLE II
COMPARISON OF DIFFERENT SPATIOTEMPORAL DATA PROCESSING SCHEMES BASED ON GEODETECTOR

Data type	Time	q statistic	p value
OD	June	0.052	0.000
	September	0.055	0.989
	October	0.084	0.002
GCD	June	0.398	0.000
	September	0.407	0.000
	October	0.385	0.000
STADD	June	0.159	0.000
	September	0.126	0.849
	October	0.289	0.000
STAD_GCD	June	0.664	0.000
	September	0.666	0.000
	October	0.664	0.000
GC_STADD	June	0.669	0.000
	September	0.671	0.000
	October	0.666	0.000

TABLE III
REGRESSION RESULTS FOR FIVE DISTINCT SPATIOTEMPORAL DATA TYPES

Variable		AICc	R^2	Adjusted R^2	Spatiotemporal Distance Ratio
OD	GTWR	138658	0.460	0.460	0.373
	GWR	140182	0.327	0.327	-
	TWR	141426	0.194	0.194	-
GCD	GTWR	138283	0.488	0.488	0.373
	GWR	139867	0.356	0.356	-
	TWR	139912	0.350	0.350	-
STADD	GTWR	39975.600	0.684	0.683	0.303
	GWR	40437.600	0.598	0.598	-
	TWR	41801.500	0.208	0.207	-
STAD_GCD	GTWR	39907.600	0.693	0.693	0.337
	GWR	40398	0.605	0.604	-
	TWR	40638.500	0.552	0.552	-
GC_STADD	GTWR	59763.100	0.699	0.699	0.373
	GWR	60446	0.620	0.619	-
	TWR	60879.900	0.559	0.559	-

4) ultimately, that a statistically significant correlation between NTLI and UCARP exists.

The research method used to detect the relationship between night-time light and residence prices from the perspective of geospatial differentiation has practical reference value and can be applied to the analysis of other residence price-related factors.

5) Nonstationary Robust Regression: To determine the bandwidth of the GTWR model, two types of fixed and adaptive methods are used. Since the spatial distribution of the community data selected in this study is not uniform, the adaptive kernel function is selected to determine the bandwidth. The AIC and the goodness of fit R^2 are selected as indicators to evaluate model confidence. The model goodness of fit refers to the degree of fit between the regression line of the sample and the observed value, that is, the ratio of the sum of the squares of the regression to the sum of the squares of the total deviations. Generally, the higher the R^2 of the model is, the better the fit of the model.

The results of the nonstationary robust regression of five different spatiotemporal datasets are shown in Table III.

The comparisons of three regressions (GWR, TWR, and GTWR) by data processing schemes, i.e., OD, GCD, STADD, STAD_GCD, and GC_STADD, show that

1) regardless of the data, the adjusted R^2 values of GTWR (0.460, 0.488, 0.693, 0.693, and 0.699) are significantly higher than those of GWR (0.327 0.356, 0.598, 0.604, and 0.619) and TWR (0.194, 0.350, 0.207, 0.552, and 0.559);
2) the adjusted R^2 values of GTWR are 0.460, 0.488, 0.683, 0.693, and 0.699 and are the highest in the same data;
3) GTWR using GC_STADD has the best regression results, with an adjusted R^2 value of 0.699.

These results show that

1) the GTWR model is more powerful in estimating the spatiotemporal heterogeneity of UCARP and NTLI and is more precise than the GWR model, which considers only spatial change, and the TWR model, which considers only time change;
2) the model fitting precision (which can be reflected using adjusted R^2 values) can be effectively improved by adding geocoding factors into the data through GeoCode;
3) the model fitting precision can be effectively improved by screening experimental data through STAD;
4) the GeoCode then STAD processes are the most robust and best of all compared methods;
5) all models indicate that a spatiotemporal correlation exists between UCARP and NTLI.

E. Discussion

Using GCD, we performed spatial heterogeneity and spatiotemporal analyses of NTLI and UCARP through GC_STADD processing.

1) From the perspective of GeoCode—similar to encoder processing in the AE—the geocoding factor M_j can effectively exaggerate economic development levels between different districts even in the same city, thus widening the economic gap within the city and improving model precision.
2) From the perspective of STAD, generally speaking, the higher NTLI is, the denser the area, the more mature the infrastructure development, the higher the level of economic development, the greater the POP density, and ultimately, the higher the residence prices. In reality, due to "nail house" and "village in the city" phenomena, some low-priced areas are found in the main urban area, while some suburbs contain high-priced villas. These villas have lower building density and darker lights than those in the main city, and these house prices are significantly higher than the prices of other buildings in the suburbs. By detecting temporal and spatial anomalies and eliminating these anomaly data, high-quality data sources for robust UCARP modeling can be obtained, so high-precision modeling can be improved.
3) Compared with simple bivariate correlation analysis, Geodetector's advantage is that it detects the relationship between NTLI and UCARP and is not limited to linearity. Without making too many assumptions, Geodetector can effectively surpass traditional statistical analysis methods and address categorical variables' limitations. Experimental results show that the NTLI data derived from the GeoCode detector can explain 67.0686% of UCARP,

which shows that NTLI is highly correlated with UCARP. The results validate the content of formula (3). Therefore, night-time light data can be used as a comprehensive indicator and a unified standard for evaluating factors related to residence prices.

4) From the perspective of the GTWR model, strong spatiotemporal heterogeneity occurs between UCARP and NTLI in Wuhan.

a) The fitting effect of the independent variable based on GC_STADD is best. This result shows that encoding independent variables while considering spatial differences can improve modeling precision. Economic development levels vary between city districts, and residence prices in each district also correspond to levels of development, whether high or low. Information such as the loop line is hidden between the city center and outskirts of the city. Therefore, partition coding the independent variables can effectively divide the space, thereby improving the interpretation of the independent variables.

b) The fitting effect of the GTWR model is better than that of the GWR and TWR models. When constructing the weight matrix, the GWR model and the TWR model consider only spatial factors or time factors separately, ignoring the whole relationship between time and space. UCARP is closely related to spatial location. Due to the trend of the real estate market and the national macro policy, time is also an important factor that impacts UCARP. Due to the heterogeneity or nonstationary of space and time, the relationship between variables varies with spatial position. GTWR considers the heterogeneity of time and space simultaneously and constructs the spatiotemporal weight matrix from two dimensions to estimate the regression coefficient of the explanatory variable so that the fitting effect is improved.

IV. Conclusion

This article chose Wuhan as the study area and UCARP data obtained by web crawler technology as the study target. Combined with Luojia1-01 NTLI data, spatiotemporal modeling (i.e., GTWR) is constructed based on GeoCode and STAD processing. Moreover, GC_STADD yielded the most robust and precise modeling results.

1) When analyzing spatial differences, we found that geographically coding variables can effectively increase the difference between district economic development levels within a city. Highlighting these differences significantly improves the explanatory power (q value from 0.052 to 0.669) of independent variables for dependent variables without adding new independent variables, which improves modeling precision.

2) When considering anomaly data, we found that STAD can effectively eliminate the nonsignificant areas and areas with opposite attributes (i.e., areas with high NTLI and low UCARP, or the converse); thus, STAD significantly and robustly improved modeling precision (R^2 from 0.460 to 0.684).

3) When we examined the nonstationarity of time and space, the small-scale NTLI modeling of UCARP based on GTWR was better than the TWR and GWR models, which significantly improved modeling precision (R^2 from 0.559 and 0.620 to 0.699).

This study's significant contributions are as follows.

This article develops the theory and methodology of spatiotemporal modeling of UCARP using Luojia1-01 NTLI, which combines the methods of geocoding, STAD, and spatiotemporal nonstationarity and allows us to propose a new spatiotemporal modeling method. Moreover, it further reveals the correlation mechanism between UCARP and NTLI.

This study is the first to apply Luojia1-01 NTLI RS data to spatiotemporal modeling and analysis of UCARP on a small scale. This new application not only extends the study on Luojia1-01 satellite data but also presents a novel approach for small-scale spatiotemporal nonstationary robust modeling and forecasting.

Future work needs to focus on the following: 1) the other variables that cannot be characterized by NTLI should be considered; and 2) could the eliminated anomaly data containing spatial differentiation be modeled?

Acknowledgment

The authors are grateful for the comments and contributions of the editors, anonymous reviewers, and the members of the editorial team. Our appreciation also goes to Wuhan University and the Hubei High Resolution Earth Observation System Data and Application Center for their provision of the Luojia1-01 NTL

References

[1] Y. Tu, H. Sun, and S.-M. Yu, "Spatial autocorrelations and urban housing market segmentation," *J. Real Estate Finance Econ.*, vol. 34, no. 3, pp. 385–406, 2007.

[2] J. R. Mellor, *Urban Sociology and Urbanized Society*. Evanston, IL, USA: Routledge, 2013.

[3] A. Tibaijuka, *Building Prosperity: Housing and Economic Development*. Evanston, IL, USA: Routledge, 2013.

[4] Z. Du and L. Zhang, "Home-purchase restriction, property tax and housing price in China: A counterfactual analysis," *J. Econometrics*, vol. 188, no. 2, pp. 558–568, 2015.

[5] H. S. Guirguis, C. I. Giannikos, and R. I. Anderson, "The US housing market: Asset pricing forecasts using time varying coefficients," *J. Real Estate Finance Econ.*, vol. 30, no. 1, pp. 33–53, 2005.

[6] N. E. Coulson and D. P. McMillen, "Estimating time, age and vintage effects in housing prices," *J. Housing Econ.*, vol. 17, no. 2, pp. 138–151, 2008.

[7] L. Wu and E. Brynjolfsson, "The future of prediction: How Google searches foreshadow housing prices and sales," in *Economic Analysis of the Digital Economy*. Chicago, IL, USA: Univ. Chicago Press, 2015, pp. 89–118.

[8] C. Liu and W. Song, "Perspectives of socio-spatial differentiation from soaring housing prices: A case study in Nanjing, China," *Sustainability*, vol. 11, no. 9, 2019, Art. no. 2627.

[9] J. Chica-Olmo, R. Cano-Guervos, and M. Chica-Rivas, "Estimation of housing price variations using spatio-temporal data," *Sustainability*, vol. 11, no. 6, 2019, Art. no. 1551.

[10] K. De Bruyne and J. Van Hove, "Explaining the spatial variation in housing prices: An economic geography approach," *Appl. Econ.*, vol. 45, no. 13, pp. 1673–1689, 2013.

[11] R. R. Brady, "The spatial diffusion of regional housing prices across US states," *Regional Sci. Urban Econ.*, vol. 46, pp. 150–166, 2014.

[12] R. F. Muth, "The spatial structure of the housing market," in *Readings in Urban Analysis*. Evanston, IL, USA: Routledge, 2017, pp. 11–26.

[13] C. Wu, X. Ye, Q. Du, and P. Luo, "Spatial effects of accessibility to parks on housing prices in Shenzhen, China," *Habitat Int.*, vol. 63, pp. 45–54, 2017.

[14] A. Einstein, *The Meaning of Relativity*. Evanston, IL, USA: Routledge, 2003.

[15] B. Huang, B. Wu, and M. Barry, "Geographically and temporally weighted regression for modeling spatio-temporal variation in house prices," *Int. J. Geographical Inf. Sci.*, vol. 24, no. 3, pp. 383–401, 2010.

[16] Z. Du, S. Wu, F. Zhang, R. Liu, and Y. Zhou, "Extending geographically and temporally weighted regression to account for both spatiotemporal heterogeneity and seasonal variations in coastal seas," *Ecological Inform.*, vol. 43, pp. 185–199, 2018.

[17] B. Wu, R. Li, and B. Huang, "A geographically and temporally weighted autoregressive model with application to housing prices," *Int. J. Geographical Inf. Sci.*, vol. 28, no. 5, pp. 1186–1204, 2014.

[18] A. S. Fotheringham, R. Crespo, and J. Yao, "Geographical and temporal weighted regression (GTWR)," *Geographical Anal.*, vol. 47, no. 4, pp. 431–452, 2015.

[19] A. S. Fotheringham, R. Crespo, and J. Yao, "Exploring, modelling and predicting spatiotemporal variations in house prices," *Ann. Regional Sci.*, vol. 54, no. 2, pp. 417–436, 2015.

[20] J. Liu, Y. Yang, S. Xu, Y. Zhao, Y. Wang, and F. Zhang, "A geographically temporal weighted regression approach with travel distance for house price estimation," *Entropy*, vol. 18, no. 8, 2016, Art. no. 303.

[21] E. Chen, Z. Ye, C. Wang, and W. Zhang, "Discovering the spatio-temporal impacts of built environment on metro ridership using smart card data," *Cities*, vol. 95, 2019, Art. no. 102359.

[22] C. Wu, F. Ren, W. Hu, and Q. Du, "Multiscale geographically and temporally weighted regression: Exploring the spatiotemporal determinants of housing prices," *Int. J. Geographical Inf. Sci.*, vol. 33, no. 3, pp. 489–511, 2019.

[23] X. Zhou, Z. Qin, Y. Zhang, L. Zhao, and Y. Song, "Quantitative estimation and spatiotemporal characteristic analysis of price deviation in China's housing market," *Sustainability*, vol. 11, no. 24, 2019, Art. no. 7232.

[24] F. Liu, M. Min, K. Zhao, and W. Hu, "Spatial-temporal variation in the impacts of urban infrastructure on housing prices in Wuhan, China," *Sustainability*, vol. 12, no. 3, 2020, Art. no. 1281.

[25] V. Stepanyan, T. Poghosyan, and A. Bibolov, *House Price Determinants in Selected Countries of the Former Soviet Union,* International Monetary Fund, Working Paper No. 2010/104, 2010.

[26] N. Miller, L. Peng, and M. Sklarz, "House prices and economic growth," *J. Real Estate Finance Econ.*, vol. 42, no. 4, pp. 522–541, 2011.

[27] H. G. Fereidouni, U. Al-Mulali, J. Y. Lee, and A. H. Mohammed, "Dynamic relationship between house prices in Malaysia's major economic regions and Singapore house prices," *Regional Stud.*, vol. 50, no. 4, pp. 657–670, 2016.

[28] T. Xu, "The relationship between interest rates, income, GDP growth and house prices," *Res. Econ. Manage.*, vol. 2, no. 1, pp. 30–37, 2017.

[29] P. Taltavull de La Paz, "Determinants of housing prices in Spanish cities," *J. Property Investment Finance*, vol. 21, no. 2, pp. 109–135, 2003.

[30] M.-C. Chen, I.-C. Tsai, and C.-O. Chang, "House prices and household income: Do they move apart? Evidence from Taiwan," *Habitat Int.*, vol. 31, no. 2, pp. 243–256, 2007.

[31] M. Fontenla, F. Gonzalez, and J. C. Navarro, "Determinants of housing expenditure in Mexico," *Appl. Econ. Lett.*, vol. 16, no. 17, pp. 1731–1734, 2009.

[32] M.-A. Lopez-Garcia, "Housing, prices and tax policy in Spain," *Spanish Econ. Rev.*, vol. 6, no. 1, pp. 29–52, 2004.

[33] F. Tajani, P. Morano, C. Torre, and F. Di Liddo, "An analysis of the influence of property tax on housing prices in the Apulia region (Italy)," *Buildings*, vol. 7, no. 3, 2017, Art. no. 67.

[34] J. G. Montalvo, "Land use regulations and house prices: An investigation for the Spanish case," *Moneda y Credito*, vol. 230, pp. 87–120, 2010.

[35] E. Candas, S. B. Kalkan, and T. Yomralioglu, "Determining the factors affecting housing prices," in *Proc. FIG Work. Week*, 2015, pp. 17–21.

[36] D. R. Capozza, P. H. Hendershott, C. Mack, and C. J. Mayer, "Determinants of real house price dynamics," National Bureau of Economic Research, 0898-2937, 2002.

[37] J. Sabal, *The Determinants of Housing Prices: The Case of Spain*. Economics, ESADE, 2005.

[38] D. Miles, "Population density, house prices and mortgage design," *Scottish J. Political Economy*, vol. 59, no. 5, pp. 444–466, 2012.

[39] B. Dachis, G. Duranton, and M. A. Turner, "The effects of land transfer taxes on real estate markets: Evidence from a natural experiment in Toronto," *J. Econ. Geography*, vol. 12, no. 2, pp. 327–354, 2011.

[40] S. C. Bourassa, M. Hoesli, D. Scognamiglio, and S. Zhang, "Land leverage and house prices," *Regional Sci. Urban Econ.*, vol. 41, no. 2, pp. 134–144, 2011.

[41] Q. Li and S. Chand, "House prices and market fundamentals in urban China," *Habitat Int.*, vol. 40, pp. 148–153, 2013.

[42] T. E. Panduro and K. L. Veie, "Classification and valuation of urban green spaces—A hedonic house price valuation," *Landscape Urban Plan.*, vol. 120, pp. 119–128, 2013.

[43] J. Dubé, M. Thériault, and F. Des Rosiers, "Commuter rail accessibility and house values: The case of the Montreal South Shore, Canada, 1992–2009," *Transp. Res. Part A, Policy Pract.*, vol. 54, pp. 49–66, 2013.

[44] O. Levkovich, J. Rouwendal, and R. Van Marwijk, "The effects of highway development on housing prices," *Transportation*, vol. 43, no. 2, pp. 379–405, 2016.

[45] L.-X. Huang, L.-J. Chen, J.-M. Hao, D.-C. Wang, L.-G. Jin, and D. Zhao, "Study on the relationship between housing price and transportation accessibility in urban district of Tianjin, China," *Theor. Empirical Res. Urban Manage.*, vol. 12, no. 2, pp. 48–63, 2017.

[46] H. Wen, Y. Xiao, E. C. Hui, and L. Zhang, "Education quality, accessibility, and housing price: Does spatial heterogeneity exist in education capitalization?," *Habitat Int.*, vol. 78, pp. 68–82, 2018.

[47] M. R. B. Liu, "The relationship between housing price and urbanization empirical study based on provincial panel data," *South China J. Econ.*, vol. 2, pp. 41–49, 2009.

[48] L. Yong-min, "The effect of urbanization on house prices: Linear or nonlinear?——Empirical study based on four panel data regression models," *J. Finance Econ.*, vol. 37, no. 4, 2011, Art. no. 14.

[49] X.-R. Wang, E. C.-M. Hui, and J.-X. Sun, "Population migration, urbanization and housing prices: Evidence from the cities in China," *Habitat Int.*, vol. 66, pp. 49–56, 2017.

[50] C. Li, L. Zou, Y. Wu, and H. Xu, "Potentiality of using luojia1-01 nighttime light imagery to estimate urban community housing price—A case study in Wuhan, China," *Sensors*, vol. 19, no. 14, 2019, Art. no. 3167.

[51] X. Li and D. Li, "Can night-time light images play a role in evaluating the Syrian Crisis?," *Int. J. Remote Sens.*, vol. 35, no. 18, pp. 6648–6661, 2014.

[52] Z. Chen et al., "A new approach for detecting urban centers and their spatial structure with nighttime light remote sensing," *IEEE Trans. Geosci. Remote Sens.*, vol. 55, no. 11, pp. 6305–6319, Nov. 2017.

[53] B. Yu et al., "Integration of nighttime light remote sensing images and taxi GPS tracking data for population surface enhancement," *Int. J. Geographical Inf. Sci.*, vol. 33, no. 4, pp. 687–706, 2019.

[54] K. Shi et al., "Spatiotemporal variations of CO2 emissions and their impact factors in China: A comparative analysis between the provincial and prefectural levels," *Appl. Energy*, vol. 233, pp. 170–181, 2019.

[55] B. Wu, B. Yu, S. Yao, Q. Wu, Z. Chen, and J. Wu, "A surface network based method for studying urban hierarchies by night time light remote sensing data," *Int. J. Geographical Inf. Sci.*, vol. 33, no. 7, pp. 1377–1398, 2019.

[56] P. C. Sutton, C. D. Elvidge, and T. Ghosh, "Estimation of gross domestic product at sub-national scales using nighttime satellite imagery," *Int. J. Ecological Econ. Statist.*, vol. 8, no. S07, pp. 5–21, 2007.

[57] C. D. Elvidge et al., "A global poverty map derived from satellite data," *Comput. Geosci.*, vol. 35, no. 8, pp. 1652–1660, Aug. 2009, doi: 10.1016/j.cageo.2009.01.009.

[58] J. Wu, Z. Wang, W. Li, and J. Peng, "Exploring factors affecting the relationship between light consumption and GDP based on DMSP/OLS nighttime satellite imagery," *Remote Sens. Environ.*, vol. 134, pp. 111–119, 2013.

[59] C. Li, Z. Huo, X. Wang, and Y. Wu, "Study on spatio-temporal modelling between NPP-VIIRS night-time light intensity and GDP for major urban agglomerations in China," *Int. J. Remote Sens.*, vol. SI, pp. 1–24, 2022.

[60] S. Amaral, A. M. Monteiro, G. Câmara, and J. Quintanilha, "DMSP/OLS night-time light imagery for urban population estimates in the Brazilian Amazon," *Int. J. Remote Sens.*, vol. 27, no. 05, pp. 855–870, 2006.

[61] L. Zhuo, T. Ichinose, J. Zheng, J. Chen, P. Shi, and X. Li, "Modelling the population density of China at the pixel level based on DMSP/OLS non-radiance-calibrated night-time light images," *Int. J. Remote Sens.*, vol. 30, no. 4, pp. 1003–1018, 2009.

[62] S. Amaral, G. Câmara, A. M. V. Monteiro, J. A. Quintanilha, and C. D. Elvidge, "Estimating population and energy consumption in Brazilian Amazonia using DMSP night-time satellite data," *Comput., Environ. Urban Syst.*, vol. 29, no. 2, pp. 179–195, 2005.

[63] T. Ma, C. Zhou, T. Pei, S. Haynie, and J. Fan, "Responses of Suomi-NPP VIIRS-derived nighttime lights to socioeconomic activity in China's cities," *Remote Sens. Lett.*, vol. 5, no. 2, pp. 165–174, 2014.

[64] A. M. Noor, V. A. Alegana, P. W. Gething, A. J. Tatem, and R. W. Snow, "Using remotely sensed night-time light as a proxy for poverty in Africa," *Popul. Health Metrics*, vol. 6, no. 1, 2008, Art. no. 5.
[65] W. Wang, H. Cheng, and L. Zhang, "Poverty assessment using DMSP/OLS night-time light satellite imagery at a provincial scale in China," *Adv. Space Res.*, vol. 49, no. 8, pp. 1253–1264, 2012.
[66] X. Li, H. Xu, X. Chen, and C. Li, "Potential of NPP-VIIRS nighttime light imagery for modeling the regional economy of China," *Remote Sens.*, vol. 5, no. 6, pp. 3057–3081, 2013.
[67] C. Mellander, J. Lobo, K. Stolarick, and Z. Matheson, "Night-time light data: A good proxy measure for economic activity?," *PLoS One*, vol. 10, no. 10, 2015, Art. no. e0139779.
[68] C. Li, G. Li, Y. Zhu, Y. Ge, and Y. Wu, "A likelihood-based spatial statistical transformation model (LBSSTM) of regional economic development using DMSP/OLS time-series nighttime light imagery," *Spatial Statist.*, vol. 21, pp. 421–439, 2017.
[69] J. Proville, D. Zavala-Araiza, and G. Wagner, "Night-time lights: A global, long term look at links to socio-economic trends," *PLoS One*, vol. 12, no. 3, 2017, Art. no. e0174610.
[70] C. Li et al., "DMSP/OLS night-time light intensity as an innovative indicator of regional sustainable development," *Int. J. Remote Sens.*, vol. 40, no. 4, pp. 1594–1613, 2019.
[71] C. He et al., "Restoring urbanization process in China in the 1990s by using non-radiance-calibrated DMSP/OLS nighttime light imagery and statistical data," *Chin. Sci. Bull.*, vol. 51, no. 13, pp. 1614–1620, 2006.
[72] Y. Zhou et al., "A global map of urban extent from nightlights," *Environ. Res. Lett.*, vol. 10, no. 5, 2015, Art. no. 054011.
[73] K. Shi, B. Yu, J. Ma, W. Cao, and Y. Cui, "Impacts of slope climbing of urban expansion on global sustainable development," *Innovation*, vol. 4, no. 6, 2023, Art. no. 100529.
[74] Z. Chen et al., "New nighttime light landscape metrics for analyzing urban-rural differentiation in economic development at township: A case study of Fujian province, China," *Appl. Geography*, vol. 150, 2023, Art. no. 102841.
[75] J. Wei, G. He, and H. Liu, "Modelling regional socio-economic parameters based on comparison of NPP/VIIRS and DMSP/OLS nighttime light imagery," *Remote Sens. Inf.*, vol. 4, pp. 28–34, 2016.
[76] G. Zhang, X. Guo, D. Li, and B. Jiang, "Evaluating the potential of LJ1-01 nighttime light data for modeling socio-economic parameters," *Sensors*, vol. 19, no. 6, 2019, Art. no. 1465.
[77] M. J. Butt, "Estimation of light pollution using satellite remote sensing and geographic information system techniques," *GISci. Remote Sens.*, vol. 49, no. 4, pp. 609–621, 2012.
[78] W. Jiang, G. He, T. Long, C. Wang, Y. Ni, and R. Ma, "Assessing light pollution in China based on nighttime light imagery," *Remote Sens.*, vol. 9, no. 2, 2017, Art. no. 135.
[79] X. Li et al., "Anisotropic characteristic of artificial light at night–Systematic investigation with VIIRS DNB multi-temporal observations," *Remote Sens. Environ.*, vol. 233, 2019, Art. no. 111357.
[80] X. Li, L. Zhao, D. Li, and H. Xu, "Mapping urban extent using Luojia 1-01 nighttime light imagery," *Sensors*, vol. 18, no. 11, 2018, Art. no. 3665.
[81] J. Wang and C. Xu, "Geodetector: Principle and prospective," *Acta Geographica Sinica*, vol. 72, no. 1, pp. 116–134, 2017.